J. Membrane Biol. 25, 93–114 (1975)

Effect of Ionic Polarizability on Electrodiffusion in Lipid Bilayer Membranes

Robert W. Bradshaw and Channing R. Robertson

Department of Chemical Engineering, Stanford University, Stanford, California 94305

Received 8 May 1975

Summary. Ion-carrier complexes and organic ions of similar size and shape have mobilities in lipid bilayer membranes which span several orders of magnitude. In this communication, an examination is made of the hypothesis that the basis for this unusually wide range of ionic mobilities is the potential energy barrier arising from image forces which selectively act on ions according to their polarizability. Using Poisson's equation to evaluate the electrostatic interaction between an ion and its surroundings, the potential energy barrier to ion transport due to image effects is computed, with the result that the potential energy barrier height depends strongly on ionic polarizability.

Theoretical membrane potential energy profile calculations are used in conjunction with the Nernst-Planck electrodiffusion equation to analyze the available mobility data for several ion-carrier complexes and lipid-soluble ions in lipid bilayer membranes. The variation among the mobilities of different ions is shown to be in agreement with theoretical predictions based on ionic polarizability and size. Furthermore, the important influence exerted by image forces on ion transport in lipid bilayer membranes compared to the frictional effect of membrane viscosity is established by contrasting available data on the activation energy of ionic conductivity with that for membrane fluidity.

List of Symbols

A	spherical conductor radius
c	ionic concentration in the membrane
c_w	ionic concentration in the aqueous solution
E	electric field strength/$(RT/\mathcal{F}L)$
e	elementary charge
F	image force
ΔH_η	activation energy for microviscosity
ΔH_k	activation energy for electrodiffusion
J	current flux
k	electrodiffusion rate constant for $\lim \psi \to 0$ defined by $J = ck\psi L\mathcal{F}$
k_s	modified electrodiffusion rate constant
L	membrane width
P	arbitrary image charge from one of Eqs. (14)–(17)
Q	ionic charge

R	gas law constant
r	ionic radius
S	sum of image charges within spherical conductor
T	absolute temperature
u	Stokes-Einstein mobility (footnote 1)

Greek Letters

α	polarizability
β	$(\varepsilon_{\mathrm{I}}-\varepsilon_{\mathrm{II}})/(\varepsilon_{\mathrm{I}}+\varepsilon_{\mathrm{II}})$
γ	*see* Fig. 2
δ	*see* Fig. 2
ε	dielectric constant
ε_0	permittivity of free space
ζ	radial space coordinate/L
η	microviscosity relative to di(18:1)-PC
θ	*see* Fig. 2
Θ	ionic charge/e
Λ	constant defined in Eq. (44)
λ	A/L
μ	Poisson's equation constant
ξ	axial space coordinate/L
P	image charge/e
ρ	space charge density/(e/L^3)
Φ	effective potential energy barrier
φ	potential energy/RT
χ	separation distance between an arbitrary charge and a charged spherical conductor
ψ	electric potential/$(RT/\mathscr{F})$
∇^2	Laplacian

Script Letters

$\mathscr{F}$	Faraday constant
$\mathscr{D}$	Stokes-Einstein diffusivity
ℓ	L/L(di(18:1)-PC)

Subscripts

C	chemical
E	electrostatic
M, N	image charge indices
Q	refers to ion (source charge)
R	refers to location of ion binding site within the membrane
I, II, III	dielectric regions

Superscript

*	denotes maximum potential energy, φ_E^*

Abbreviations

$TPhB^-$	tetraphenylboride anion
DPA^-	dipicrylamine anion
$CCCP^-$	carbonylcyanide *m*-chlorophenylhydrazone anion
egg PC	phosphatidyl choline from egg yolk
di(N:1)-PC	diacylphosphatidyl choline of an N-carbon mono-unsaturated fatty acid
GMO	glyceryl monooleate
GMER	glyceryl monoerucin
CHL	cholesterol
PI	phosphatidyl inositol
PS	phosphatidyl serine
DPPC	dipalmitoyl phosphatidyl choline
BPE	bacterial phosphatidyl ethanolamine
PE	phosphatidyl ethanolamine

The effect of dielectric polarization on a charge near an interface, commonly referred to as the image force, on the ionic permeability of thin membranes has been shown to be important in lipid bilayer membranes [1, 19, 20, 28] and in ultrathin polymeric reverse osmosis membranes [2]. Although previous theoretical treatments of electrodiffusion have represented ions as point charges for image force calculations [19, 28], this assumption is questionable for large ions such as ion-carrier complexes and organic ions within lipid bilayer membranes since these structures are typically less than 50 Å thick. Andersen and Fuchs [1] recognized this point, although they employed the point charge image force in analyzing the current-voltage characteristic of tetraphenylboride transport. The finite size of an ion manifests itself in electrostatic interactions through the property of polarizability, a quantity which depends on chemical structure as well as ionic dimensions. Polarizability has been shown to be significant in describing specificity effects among ions of the same charge for ionic conductivity in polymers [3] and zeolite ion exchangers [4] and association equilibria between metal ions and complexing agents such as valinomycin and the macrotetralide actins [24, 33]. Parsegian [29] and Tredgold [38] have also studied the effects of ionic size on the equilibrium properties of ionic partition and hydration energy.

In this communication, the importance of ionic polarizability and size in the electrodiffusion of single ions within lipid bilayer membranes is considered and is shown to account for the selectivity observed in ionic mobilities among ion-carrier complexes and lipid-soluble ions. The approach herein parallels previous analyses of electrodiffusion in thin membranes based on Poisson's equation for determining the image force

which retards ionic migration and on the Nernst-Planck equation as the phenomenological relation between ion flux and driving forces. An approximate solution is given for the image force, or equivalently, the potential energy barrier confronting an ion within the membrane, which simplifies the computations considerably and corresponds closely to the exact solution. To evaluate the significance of ion-specific electrostatic effects, theoretical calculations of ionic mobilities are carried out using ionic polarizability and size data reported for ions whose mobilities in lipid bilayer membranes are available.

Theoretical Considerations

Electrodiffusion in lipid bilayer membranes may be described by the Nernst-Planck equation, and as such, the current flux, J, for a single univalent ionic specie soluble in a membrane bounded by identical aqueous solutions is given by [1, 9, 18, 20, 28]

$$J = 2\frac{\mathscr{F} c_w \mathscr{D}}{L} \frac{\sinh(\psi/2)}{\int_{\xi_R}^{1-\xi_R} e^{\psi s} e^{\varphi(s)} ds} \tag{1}$$

where $\mathscr{F}$ is the Faraday constant, c_w is the ionic concentration in the aqueous phase adjacent to the membrane, ξ_R and $1-\xi_R$ are the locations of the internal membrane binding sites, $\mathscr{D}$ is the ionic diffusivity computed using the Stokes-Einstein relation and L is the membrane width. The dimensionless variables for distance from the interface, ξ, electric potential, ψ, and potential energy, φ, have been normalized by the dimensional quantities L, $(RT/\mathscr{F})$ and RT, respectively.

The potential energy function within the membrane, $\varphi(s)$, may be resolved into a position-independent component, φ_C, due to short-range chemical forces affecting solubility, and a position-dependent component, $\varphi_E(\xi)$, due to long-range electrostatic interactions [23]. The Nernst-Planck equation may then be written as

$$J = \frac{2\mathscr{F} c \mathscr{D}}{L} \frac{\sinh(\psi/2)}{\int_{\xi_R}^{1-\xi_R} e^{\psi s} e^{\varphi_E(s)} ds} \tag{2}$$

where $c = c_w \exp(-\varphi_C)$ is the ionic concentration at the binding sites within the membrane, located at ξ_R and $1-\xi_R$. Here, the term, $\exp(-\varphi_C)$, assumes the role of a partition coefficient. Eq. (2) implies that the membrane

conductivity, $[(J/\psi)\cdot(RT/\mathscr{F})]$, depends on two distinct quantities, the population of charge carriers in the membrane and their mobility under the influence of an external force. Mobility is usually reported as an electrodiffusion rate constant, k, which in the limit of low applied voltages $(\psi \to 0)$ is[1]

$$k = \frac{\mathscr{D}}{L^2} \frac{1}{\int_{\xi_R}^{1-\xi_R} e^{\varphi_E(s)} ds}. \tag{3}$$

This form will be used subsequently to interpret available ion transport data.

Electrostatic Effects

The potential energy barrier associated with image forces attracting an ion within a thin membrane toward the interfaces may be obtained by solving Poisson's equation for the electrical potential using simple dielectric models for the membrane, the surrounding solutions and the ion. The membrane is idealized as a homogeneous film having a dielectric constant, ε, of 2.1, while the surrounding solutions are assumed to be either perfect conductors [19] or dielectric regions having a dielectric constant of 78.1 [28]. An ion having a charge, Q, and polarizability, α, is represented by an electrostatically equivalent spherical conductor having a radius, A, where according to Böttcher [8], $\alpha = A^3$. Since ions are not perfectly polarizable, the actual dimensions of any given ion will always exceed A. Nonspherical ions may be represented as spheres for electrostatic calculations provided that the mean polarizability of the tensorial components is used [8].

The system considered is illustrated in Fig. 1 along with a dimensionless cylindrical coordinate system constructed about an axis which passes through the center of an ion embedded within the membrane and is perpendicular to the interfaces. The electrostatic potential problem obtained by applying Poisson's equation to the membrane (II) and surrounding solutions (I, III) becomes

$$\nabla^2 \psi_{II} = -4\pi \frac{\mu}{\varepsilon_{II}} \rho(\xi, \zeta) \tag{4}$$

$$\nabla^2 \psi_{I,III} = 0 \tag{5}$$

1 The Stokes-Einstein mobility u, given by $\mathscr{D} = uRT$, is related to the electrodiffusion rate constant, k, as follows: $u = kL^2RT$.

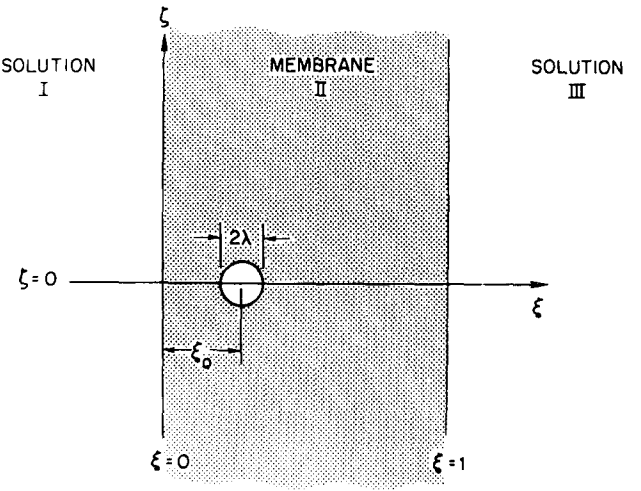

Fig. 1. Schematic diagram of a lipid bilayer membrane showing the cylindrical coordinate system used in the electrostatic potential calculations

where

$$\mu = \frac{e}{4\pi\varepsilon_0 L\left(\frac{RT}{\mathscr{F}}\right)} \tag{6}$$

and the dimensionless space charge distribution is given by $\rho = \Theta$ for $\xi = \xi_Q$ and $\zeta = 0$, and $\rho = 0$ for $\xi \neq \xi_Q$ and all ζ, where $\Theta = Q/e$.

The interfacial boundary conditions are [34]

$$\varepsilon_i \frac{\partial \psi_i}{\partial \xi} = \varepsilon_{\mathrm{II}} \frac{\partial \psi_{\mathrm{II}}}{\partial \xi} \qquad i = \mathrm{I}, \mathrm{III} \tag{7}$$

$$\frac{\partial \psi_i}{\partial \zeta} = \frac{\partial \psi_{\mathrm{II}}}{\partial \zeta} \qquad i = \mathrm{I}, \mathrm{III} \tag{8}$$

at $\zeta = 0, 1$. The presence of a spherical conductor requires an additional boundary condition, namely, that the surface of the sphere be equipotential [34]. Thus, for a spherical conductor positioned entirely within the membrane

$$\psi_{\mathrm{II}} = \text{constant on } \lambda^2 = \zeta^2 + (\xi - \xi_Q)^2 \tag{9}$$

where $\lambda = A/L$.

Neumcke and Läuger [28] solved the point charge problem, Eqs. (4)–(8), by the method of images for dielectric surroundings, whereas Haydon and Hladky [19] considered the surroundings to be perfect conductors in which case the dielectric constant is essentially infinite. Only a small

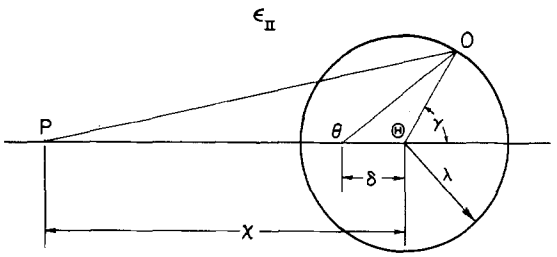

Fig. 2. Geometrical construction considered for examining the condition of equipotentiality at the surface of a charged spherical conductor polarized by an external charge

difference ($\sim 5\%$) is observed between the image potential calculations performed by these workers since in both cases the membrane dielectric constant is much less than that of the surroundings. The solutions obtained, in either instance, for the point charge problem provide the basis for analyzing the electrostatics of a spherical conductor ion in the following section.

Results

Exact Solution

In the presence of a spherical conductor, the image charges arising from the dimensionless source charge, Θ, which satisfy the interfacial boundary conditions, Eqs. (7) and (8), disturb the equipotential condition at the surface of the sphere, Eq. (9), thereby requiring additional compensatory image charges. Before discussing the solution of the thin membrane problem, the mathematical procedure used herein is best illustrated by a simpler problem which considers the polarization of a conducting sphere embedded in a uniform dielectric medium.

Let P be an arbitrary charge separated from the center of a charged spherical conductor by a distance, χ. Referring to Fig. 2, a charge, θ, is placed at a distance, δ, from the center of the sphere to restore equipotentiality at the surface. At any arbitrary point, O, on the surface,

$$\psi = \frac{\mu}{\varepsilon_{II}} \left\{ \frac{\Theta}{\lambda} + \frac{\theta}{(\delta^2 + \lambda^2 + 2\lambda\delta\cos\gamma)^{1/2}} + \frac{\mathrm{P}}{(\chi^2 + \lambda^2 + 2\lambda\chi\cos\gamma)^{1/2}} \right\}. \quad (10)$$

Following Smythe [34], let

$$\delta = \lambda^2/\chi \quad (11)$$

then

$$\psi = \frac{\mu}{\varepsilon_{II}} \left\{ \frac{\Theta}{\lambda} + \frac{P + \frac{\chi}{\lambda}\theta}{(\chi^2 + \lambda^2 + 2\lambda\chi\cos\gamma)^{1/2}} \right\}; \tag{12}$$

hence, if

$$\theta = -P\lambda/\chi \tag{13}$$

the potential on the surface is independent of γ.

A procedure for solving Eqs. (4)–(9) may be formulated based on the foregoing algorithm and the corresponding solution for a point charge ion in a thin membrane. An ion located at $(\xi, \zeta) = (\xi_Q, 0)$ requires that the image charges

$$P_{-N} = -\beta^{2N-1}\Theta \quad \text{at} \quad \xi = -(2(N-1) + \xi_Q); \quad N = 1, 2, 3 \ldots \tag{14}$$

$$P'_{-N} = \beta^{2N}\Theta \quad \text{at} \quad \xi = -(2N - \xi_Q); \quad N = 1, 2, 3 \ldots \tag{15}$$

$$P_N = -\beta^{2N-1}\Theta \quad \text{at} \quad \xi = 2N - \xi_Q; \quad N = 1, 2, 3 \ldots \tag{16}$$

$$P'_N = \beta^{2N}\Theta \quad \text{at} \quad \xi = 2N + \xi_Q; \quad N = 1, 2, 3 \ldots \tag{17}$$

where

$$\beta = (\varepsilon_I - \varepsilon_{II})/(\varepsilon_I + \varepsilon_{II}) \tag{18}$$

be placed in the surroundings to satisfy the interfacial boundary conditions [28]. The images denoted by primes [Eqs. (15) and (17)] are not potential-determining for a point charge [28], but do affect a spherical conductor.

The above image charges disturb the equipotential state at the surface of the sphere and must be compensated for by adding images as indicated by Eqs. (11) and (13). Subsequently, each image charge in the sphere requires new sets of images in the surroundings given by Eqs. (14)–(17), where ξ_Q is replaced by the location of the image charge, θ, in the sphere to satisfy the interfacial boundary conditions. This method of successive approximations may be pursued to satisfy both interfacial and sphere surface boundary conditions to the desired level of accuracy. The calculation is convergent since the requisite image charges become progressively smaller in magnitude and those in the surroundings progressively recede from the sphere as well.

If $S(\xi)$ is the sum of all the image charges placed within the sphere located at position ξ, the image force, F, acting on the spherical ion is [34]

$$\frac{F}{\frac{e}{L}\left(\frac{RT}{\mathscr{F}}\right)} = \frac{\mu\Theta}{2\varepsilon_{II}\lambda}\frac{dS}{d\xi}. \tag{19}$$

The potential energy is easily obtained by integrating Eq. (19) with the result that

$$\varphi_E(\xi_Q) = -\frac{\mu\Theta}{2\varepsilon_{II}\lambda}\{S(\xi_Q) - S(\xi_R)\} \tag{20}$$

where ξ_R, the ion binding site location, is taken as the reference position for potential energy [18, 20].

The above procedure for calculating potential energy profiles may be implemented on a digital computer and will be referred to subsequently as the exact solution of Eqs. (4)-(9). An approximate solution for the image potential, φ_E, would be more convenient for data analysis and parametric studies of ion transport in lipid bilayer membranes. The exact solution, therefore, is regarded as the measure against which approximate potential energy calculations will be tested.

Approximate Solution

As an initial simplification, suppose that the only interfacial boundary condition considered pertains to the interface between the sphere and an arbitrary image charge in the surroundings, P_N, [Eqs. (14)-(17)] and that the other interface is neglected. The equipotentiality condition at the surface of the sphere is retained. The first step in this approximation to the electrostatics problem is illustrated in Fig. 3. The compensatory image charge, $\theta_1 = -P_N\lambda/\chi_N$, is located within the sphere at $\xi_1 = \xi_Q - \lambda^2/\chi_N$ to

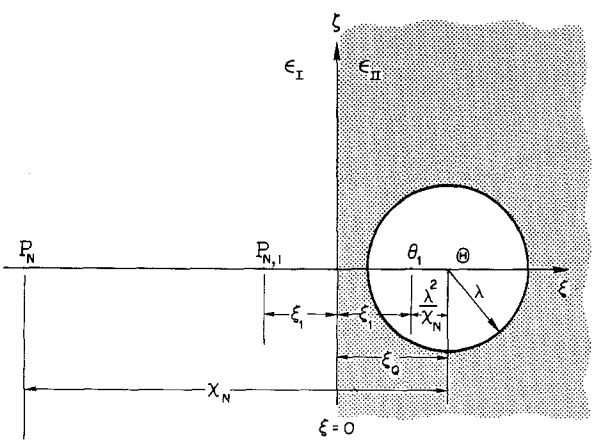

Fig. 3. Locations of selected image charges for a charged spherical conductor near the interface separating two dissimilar dielectric regions

satisfy the equipotential surface condition. Since the far interface ($\xi = 1$ for the situation shown) is neglected, only one image charge, $P_{N,1}$, is needed to satisfy the interfacial conditions at $\xi = 0$ where $P_{N,1} = -\beta\theta_1$ [28].

Further corrections to both the interfacial and surface boundary conditions follow from the method of successive approximations developed for the exact solution and may be stated in terms of the following recursion relations

$$\theta_{M+1} = -\frac{\lambda}{\xi_Q + \xi_M} P_{N,M} \tag{21}$$

$$P_{N,M} = -\beta\theta_M \tag{22}$$

$$\xi_{M+1} = \xi_Q - \frac{\lambda}{\xi_Q + \xi_M} \tag{23}$$

with the initial conditions,

$$P_{N,0} = P_N \tag{24}$$

$$\xi_0 = \chi_N - \xi_Q. \tag{25}$$

Eqs. (21)–(23) reduce to

$$\frac{\beta^{M+1}}{\theta_{M+1}} + \frac{\beta^{M-1}}{\theta_{M-1}} = 2\left(\frac{\xi_Q}{\lambda}\right)\frac{\beta^M}{\theta_M}. \tag{26}$$

By noting the similarity between Eq. (26) and the hyperbolic identities

$$\sinh(M+1)\,y + \sinh(M-1)\,y = 2\cosh y \sinh My \tag{27}$$

$$\cosh(M+1)\,y + \cosh(M-1)\,y = 2\cosh y \cosh My \tag{28}$$

and by assigning

$$\cosh y = \xi_Q/\lambda \tag{29}$$

then the form of the general solution becomes

$$\frac{\beta^M}{\theta_M} = x_1 \cosh My + x_2 \sinh My. \tag{30}$$

Evaluation of the constants, x_1 and x_2, from the initial conditions gives

$$x_1 = -\frac{\beta}{P_N} \tag{31}$$

$$x_2 = -\frac{\beta}{P_N}\,\frac{\chi_N - \xi_Q}{\lambda \sinh y}. \tag{32}$$

Accordingly, the total charge appearing in the sphere due to an arbitrary image charge, P_N, from Eqs. (14)-(17) is

$$S=\sum_{M=1}^{\infty}\theta_M=-P_N\sum_{M=1}^{\infty}\frac{\beta^{M-1}\sinh y}{\cosh My\sinh y+\left(\frac{\chi_N-\xi_Q}{\lambda}\right)\sinh My}. \tag{33}$$

The potential energy due to a particular image of the source charge is then given by Eqs. (20) and (33) and the hyperbolic recursion relations, Eqs. (27) and (28). The total potential energy is simply the sum of the contributions of all the image charges in Eqs. (14)-(17).

Considering an ion whose position is bounded by $0\leqq\xi\leqq 1/2$, the most important image charge is that nearest the source charge, P_{-1}, (Eq. 14). Since $P_{-0}=-\beta\Theta$ and $\chi_{-0}=2\xi_Q$, $(\chi_{-0}-\xi_Q)/\lambda=\cosh y$ and given the identity

$$\sinh(M+1)y=\sinh y\cosh My+\cosh y\sinh My, \tag{34}$$

Eq. (33) becomes

$$S=\Theta\sum_{M=1}^{\infty}\frac{\beta^M\sinh y}{\sinh(M+1)y}. \tag{35}$$

The potential energy function may be obtained as indicated previously (Eq. 20). This result corresponds to a membrane which is semi-infinite in the positive ξ direction. It may be shown to reduce to the analogous result of Neumcke and Läuger [28] for a point charge residing in a semi-infinite membrane (Eq. 27 of their paper) as λ approaches zero. This result is also presented by Smythe [34].

If the next nearest image charge, P_1, is included in the potential energy computation, the result is

$$S=\Theta\sum_{M=1}^{\infty}\beta^M\left\{\frac{\sinh y_1}{\sinh(M+1)y_1}-\frac{\sinh y_2}{\sinh(M+1)y_2}\right\} \tag{36}$$

where $\cosh y_1=\xi_Q/\lambda$ and $\cosh y_2=(1-\xi_Q)/\lambda$ since P_1 is the reflection of the ionic charge about the interface at $\xi=1$. Eq. (36) is symmetrical about the mid-plane of the membrane as the nature of the problem dictates and is therefore a significant improvement over Eq. (35). Hereafter, Eq. (36) will be referred to as the approximate solution.

Numerical Calculations

Potential energy calculations using the exact solution are compared with the approximate solution (Eq. 36) and those for a semi-infinite

Table 1. Comparative electrostatic potential energy calculations

	Position (ξ)				
	0.1	0.2	0.3	0.4	0.5
Exact	12.94	26.02	29.26	30.49	30.83
Approximate	12.89	25.84	29.01	30.20	30.52
Semi-infinite	12.95	26.14	29.63	31.24	32.18

$L=40$ Å; $A=2$ Å; $\xi_R L=3$ Å; $\varepsilon_{I,III}\to\infty$.

membrane (Eq. 35) in Table 1 for typical values of membrane and ionic parameters. The semi-infinite membrane values differ by about 10 % from the exact value while the approximate solution is always within about 1 % of the exact result. Evidently, the approximate solution, based on only the two image charges nearest the ion, is an accurate substitute for the exact solution. Subsequent potential energy calculations will employ the approximate solution exclusively.

In agreement with the results of Neumcke and Läuger [28] for a point charge, the potential energy function is relatively insensitive to the membrane width for values characteristic of lipid bilayer membranes. To cite a representative case, an ion having a polarizability of 8 Å^3 ($A=2$ Å) and bound an equal distance from the interface in each of several membranes

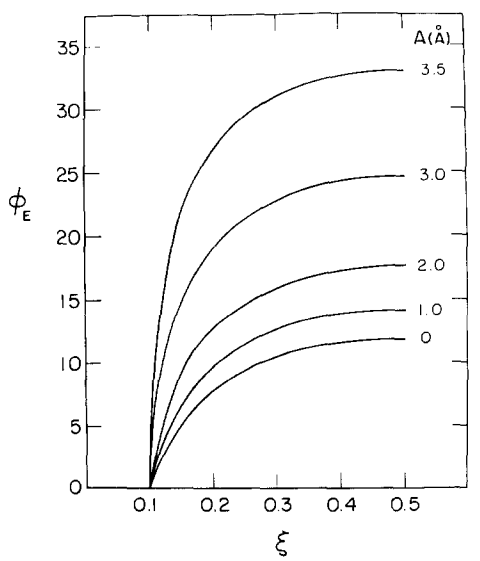

Fig. 4. Electrostatic potential energy profiles of polarizable univalent ions for several values of the radius of the equivalent charged spherical conductor. $L=40$ Å; $\xi_R L=4$ Å; $\varepsilon_{I,III}\to\infty$

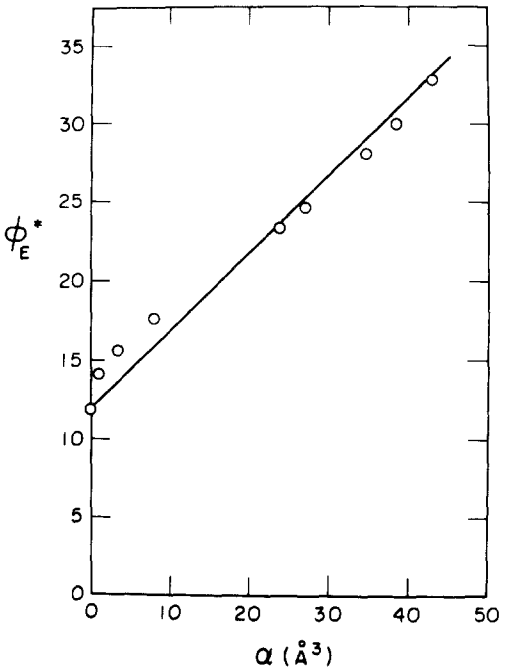

Fig. 5. The effect of ionic polarizability on the maximum value of the electrostatic potential energy barrier. $L=40$ Å; $\xi_R L=4$ Å; $\varepsilon_{I,III}\to\infty$

such that $\xi_R L=3$ Å, yields peak or maximum potential energies, φ_E^*, of 28.7, 30.5, 31.6 and 32.3 for membrane widths of 30, 40, 50 and 60 Å, respectively.

Polarizability, expressed as the radius of the equivalent spherical conductor, affects the peak potential energy quite markedly as shown in Fig. 4. Polarizability will therefore significantly influence ion transport rates in bilayer membranes since the potential energy appears as an exponential coefficient in the Nernst-Planck equation. The asymptotic case of $A=0$, corresponding to a point charge ion, concurs with the results of Neumcke and Läuger [28].

The relationship between maximum potential energy, φ_E^*, and polarizability, α, is depicted in Fig. 5. The linearity of this graph is a consequence of two energetic contributions to the total electrostatic potential energy. The φ_E^* intercept at $\alpha=0$ corresponds to the point charge problem and represents the energy required to overcome the image forces attracting the central ionic charge toward the interfaces. The slope is associated with the polarization energy arising from the action of the image charges in the surroundings on the spherical conductor. Recalling that the polarization

energy of a body in an electrical field of strength, E, is [8]

$$\varphi_{\text{polarization}} = -\frac{1}{2}\frac{\alpha}{L^3}E^2 \tag{37}$$

it follows that

$$\varphi_E^* = \varphi_E^*|_{\alpha=0} + \frac{\alpha}{2L^3}(E^2|_{\xi=\xi_R} - E^2|_{\xi=1/2}). \tag{38}$$

Eq. (38) provides a simple correlation between peak potential energy and ionic polarizability and thus further reduces the computational requirements when comparing ion transport phenomena for a large number of ions.

Discussion

The purpose of considering electrostatic effects due to ionic polarizability on ion transport phenomena in lipid bilayer membranes, in addition to charge, is to provide a basis for interpreting experimentally measured ionic mobilities, given by the electrodiffusion rate constant, k. The theoretical potential energy calculations presented in the preceding section permit ionic mobilities to be determined for ions whose polarizabilities are known so that comparisons may be made with electrodiffusion measurements in lipid bilayer membranes. Published data on ionic mobilities in bilayer membranes are presented in Table 2, together with the pertinent characteristics of the ions and membranes studied.

A striking feature of Table 2 is the great disparity among mobilities for these ions of similar size and shape. Furthermore, the usual inverse relationship between mobility and hydrodynamic radius given by the Stokes-Einstein equation for viscous fluids is reversed in the case of the carrier-cation complexes in comparison with the lipid-soluble ions, tetraphenylboride ($TPhB^-$) and dipicrylamine (DPA^-). However, the inverse relationship between electrodiffusion rate constants (k) and ionic polarizabilities (α), for the hydrodynamically similar lipid-soluble ions, $TPhB^-$, DPA^-, and carbonyl cyanide m-chlorophenylhydrazone ($CCCP^-$), is consistent with the previous discussion concerning the increase in height of the image potential energy barrier to electrodiffusion which results from an increase in ionic polarizability.[2]

The influence of polarizability on ionic mobility may be evaluated quantitatively by rewriting Eq. (3) in a form which explicitly identifies

2 Increasing ionic polarizability decreases the Born energy which primarily affects ionic partition rather than mobility.

Table 2. Ionic properties and electrodiffusion rate constants for polarizable ions in lipid bilayer membranes

Ion	Shape, Size	Polarizability ($Å^3$)	k (sec^{-1})	Membrane	L (Å)	η
$TPhB^-$	Sphere [13] $r=4.2$ Å [a]	44.5 [17]	9 [23]	di(18:1)-PC	42 [11] 48 [33]	1
$TPhB^-$	see above	see above	2.5×10^2 [1]	BPE	30 [1]	1
DPA^-	Ellipsoid $r=3,5$ Å	38.4 [b] 35.2 [16]	3.8×10^2 [23]	di(18:1)-PC	see above	1
$CCCP^-$	Cylinder $r=2.5$ Å $h=8$ Å	23 [b]	4.3×10^3 [27]	egg PC-CHL (1:1)	47 [26]	3 [22] 10 [10]
Trinactin-NH_4^+	Sphere [33] $r=6.2$ Å [c] $r=4$ Å [d]	75 [b]	1.5×10^4 [21]	GMO	33 [e] [12]	1 [10]
Trinactin-K^+	see above	see above	2.3×10^4 [21]	GMO	see above	see above
Trinactin-NH_4^+	see above	see above	5.0×10^3 [37]	GMO	48 [f] [12]	1 [10]
Trinactin-NH_4^+	see above	see above	8.0×10^3 [5]	GMO	48 [f] [12]	1 [10]
Trinactin-NH_4^+	see above	see above	4.0×10^3 [5]	GMER	56 [g]	1 (est.)
Valinomycin-K^+	Cylinder [33] $r=7.5$ Å $h=12$ Å	140 [b]	1.5×10^4 [15, 36]	PI, PS	55 [35]	1

[a] Stokes radius in methanol.
[b] Estimated from Ref. [7].
[c] Crystal radius from Ref. [33].
[d] Stokes radius in acetonitrile from Ref. [31].
[e] *n*-hexadecane solvent.
[f] *n*-decane solvent.
[g] Based on di(22:1)-PC from Ref. [35].

the two components of the electrodiffusion energy barrier, namely the contribution due to electrostatic forces and that due to membrane viscosity. Defining the effective electrostatic potential energy barrier, Φ_E, to be given by

$$\exp(\Phi_E) = \int_{\xi_R}^{1-\xi_R} e^{\varphi_E(s)}\, ds \tag{39}$$

and noting that the Stokes-Einstein diffusivity, $\mathscr{D}$, may be written as

$$\mathscr{D} = \mathscr{D}_o \exp[-\Delta H_\eta / RT] \tag{40}$$

where ΔH_η is the activation energy for membrane microviscosity, then Eq. (3) becomes

$$k = \frac{\mathscr{D}_o}{L^2} \exp\left\{-\frac{\Delta H_\eta}{RT} - \Phi_E\right\}. \tag{41}$$

Eq. (41) may be used to correlate the measured electrodiffusion rate constants, k, given in Table 2 with effective electrostatic potential energies, Φ_E, obtained using Eqs. (20), (36) and (39). Although the value $\mathscr{D}_o$ appearing in Eq. (41) is not known precisely, it may be expected to vary by less than a factor of two for the range of ionic sizes considered herein. Furthermore, the variance in the diffusivity of the ions due to variations in the microviscosity, η, (normalized with respect to dioleoyllecithin) among the several membrane materials listed in Table 2 may be accounted for by using the Stokes-Einstein equation when comparing electrodiffusion rate constants, k, for different ions. As shown in Table 2, membranes for which this correction is significant incorporate cholesterol. For example, Cogan *et al.* [10] observed an order of magnitude increase in microviscosity for the mixed lipid, egg-PC-CHL, compared to the phospholipid alone, while for the same system Jacobsen and Wobschall [22] report a factor of three increase in microviscosity. Szabo [37] observed a factor of five decrease in the mobility of the trinactin-NH_4^+ complex in GMO-CHL(1:1) membranes in comparison with GMO membranes. Therefore, the microviscosity of egg PC-CHL(1:1) membranes relative to di(18:1)-PC membranes is assumed to be five in subsequent calculations. Because of these differences in ionic diffusivity, $\mathscr{D}$, due to variations in membrane microviscosity, it is convenient to define a modified electrodiffusion rate constant, k_s, as follows

$$k_s = k\eta\ell^2 \tag{42}$$

where ℓ is the membrane width normalized with respect to the average di(18:1)-PC width from Table 2. Combining Eqs. (41) and (42) gives

$$k_s = \Lambda \exp(-\Phi_E) \tag{43}$$

where, using Eq. (40), Λ is given by

$$\Lambda = \frac{\mathscr{D}\eta}{L^2_{\text{di(18:1)-PC}}}. \tag{44}$$

Note that Λ is a constant, since the product $\mathscr{D}\eta$ is a constant according to the Stokes-Einstein relation. Consequently, Eq. (43) may be used to correlate electrodiffusion rate constants with theoretically determined values of the electrostatic potential energy barrier, Φ_E.

Values of the effective electrostatic potential energy, Φ_E, were calculated using Eqs. (20) and (36) together with the values of α and L in Table 2. The values of α were calculated according to the functional group additivity rule using extensive tabulations from Bondi [7] except for $TPhB^-$ and

Table 3. Electrodiffusion rate constants and theoretical energy barrier calculations for several polarizable ions in lipid bilayer membranes

Ion	k_s (sec^{-1})	$\xi_R L$ (Å)	Φ_E	φ_E^*
$TPhB^-$ □	9	4.2	27.7	28.9
$TPhB^-$ ○	1.1×10^2	4.2	24.8	26.3
DPA^- △	3.8×10^2	4.2	24.6	25.8
$CCCP^-$ ◇	2.3×10^4	4.2	20.3	21.5
Trinactin-NH_4^+ ●	8.0×10^3	5.0	20.1	21.4
Trinactin-K^+ ■	1.2×10^4	5.0	20.1	21.4
Trinactin-NH_4^+ ▲	5.7×10^3	5.0	22.5	23.7
Trinactin-NH_4^+ ◆	9.0×10^3	5.0	22.5	23.7
Trinactin-NH_4^+ ⊕	6.2×10^3	5.0	23.2	24.3
Valinomycin-K^+ ⊹	3.3×10^4	6.0	19.7	20.9

$\varepsilon_I, \varepsilon_{III} \to \infty$.

DPA^- for which experimental measurements are available [16, 17]. The surrounding solutions were assumed to be perfect conductors and as indicated in Table 3, the ionic binding sites were assumed to be located at one ionic radius within the membrane [1, 20, 28]. The values of k, η and L from Table 2 were used to compute the modified electrodiffusion rate constant, k_s, according to Eq. (42), and the relationship between k_s and the corresponding value of the effective electrostatic potential energy barrier, Φ_E, for each ion-membrane system considered herein is shown in Fig. 6. These values of k_s and Φ_E are presented in Table 3 as are the values of φ_E^*, this latter quantity also serving to correlate the mobility data. This follows from the fact that the major contribution to the integrand in Eq. (39) can be attributed to values of $\varphi_E(s)$ which are close to the maximal value, consequently, $\varphi_E^* \doteq \Phi_E$.

The correlation between the electrostatic potential energy barrier, Φ_E, and the modified electrodiffusion rate constant, k_s, shows reasonable agreement with the image force theory discussed herein. The solid line shown in Fig. 6 was obtained using a linear least-squares analysis of Eq. (43) with the data for k_s and Φ_E given in Table 3. The equation of this line is $\ln k_s = 29.3 - 0.96\,\Phi_E$, which indicates that the correlation is in good agreement with the theoretical slope of unity.

The values of the effective electrostatic potential energy, Φ_E, are sensitive to the location of the ion binding site, ξ_R. This sensitivity between Φ_E and ξ_R may be attributed to the fact that the image force increases rapidly and without bound as an ion approaches the membrane/solution interface and thus exerts a strong influence on the magnitude of the electrostatic potential energy given by the integral of the image force [Eqs. (19)

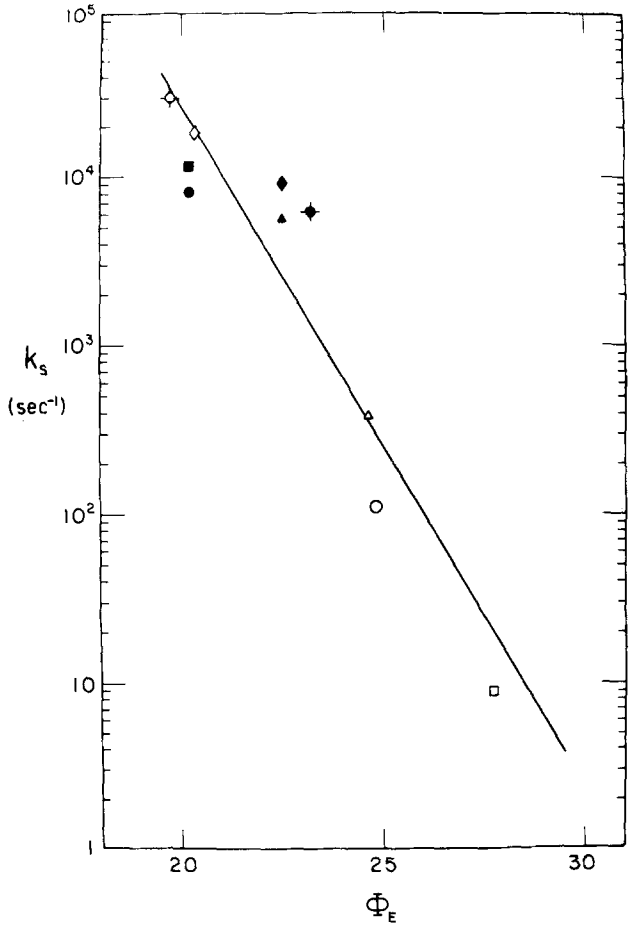

Fig. 6. The relation between the electrodiffusion rate constants of several polarizable ions observed in lipid bilayer membranes and theoretical calculations of the potential energy barrier due to image forces. The least-squares fit to the data given by $\ln k_s = 29.3 - 0.96\,\Phi_E$

and (20)]. This degree of parametric sensitivity to the choice of ξ_R is displayed by both polarizable and point charge ions and suggests that refinements may be necessary in the simple membrane model employed herein and elsewhere [1, 19, 28] in treating image effects in lipid bilayer membranes. One possible refinement would be to recognize the structural differences between the polar head groups of membranes formed from phospholipids and glycerolipids, respectively, by using a more detailed dielectric model of the membrane.

As a further confirmation of the importance of ionic polarizability on electrodiffusion in lipid bilayer membranes, consider the activation energy

Table 4. Activation energies for microviscosity in lipid bilayer membranes

Lipid	$\Delta H_\eta/RT$	Reference
egg PC	12.0	[10], [22]
egg PC	13.3	[32]
egg PC	11.5	[39]
DPPC	16.5	[40]
DPPC	14.8	[14]
DPPC-CHL(1:1)	21.0	[14]
DPPC-CHL(1:1)	10.2	[40]
egg PC-CHL(1·2:1)	8.2	[22]
egg PC-CHL(1·5:1)	14.3	[10]

for the electrodiffusion rate constant, $\Delta H_k/RT$, where from Eq. (41)

$$\frac{\Delta H_k}{RT} = \Phi_E + \frac{\Delta H_\eta}{RT}. \tag{45}$$

Benz and Stark [5] have recently reported a value of 33 for the electrodiffusion activation energy, $\Delta H_k/RT$, for the trinactin-NH_4^+ complex in GMO membranes. This value agrees very well with that computed from Eq. (45) using the value of Φ_E for this particular complex and membrane from Table 3 and the microviscosity activation energy, $\Delta H_\eta/RT$, as given in Table 4. These values are 22 and 13, respectively. In contrast, if an ion is regarded as a point charge, $\alpha = 0$, then for the same conditions used in the potential energy calculations for trinactin-NH_4^+, namely, $\xi_R L = 5.0$ Å, ε_I, $\varepsilon_{III} \to \infty$, the value for the effective electrostatic potential energy is 8.5, which clearly underestimates the measured value of 33.

It is apparent from the foregoing discussion that ionic polarizability is a significant parameter in describing the effect of image forces on ionic mobility in lipid bilayer membranes. The good agreement between the experimental values of k_s and the theoretical results for Φ_E according to $\ln k_s = \ln A - \Phi_E$ indicates that the image force model discussed herein yields an accurate estimate of the difference between the potential energy barriers which confront different ions within lipid bilayer membranes. The fact that only moderate agreement is achieved between the correlation intercept, $\ln A = 29.3$ and the value of $\ln A$ computed using data in the literature,[3] suggests that further refinements in the analysis of electrodiffusion in bilayer membranes may be needed.

3 The value of $\ln A \doteq 13$ may be computed from Eq. (44) using the values, $L_{\text{di(18:1)-PC}} = 45$ Å, $\eta = 1$ and $\mathscr{D} \doteq 10^{-7}$ cm^2/sec. This value of the diffusivity is that measured in egg PC bilayers for the neutral molecule, pyrene [39], which is dimensionally similar to the ions considered herein.

Conclusions

A primary goal of model membrane studies of the kind discussed herein is to understand the relationship between membrane structure and ionic permeability in a comparatively simple system about which a considerable amount of information describing the structural characteristics of both membrane and ionic permeants exists. The ability of a membrane to discriminate among a variety of possible permeants is essentially due to two factors, the mobility and the solubility of the permeants in the membrane. This communication is concerned with the relationship between ionic mobility and electrostatic polarization forces acting on ions in thin membranes. It is important to recognize that the magnitude of the polarization forces depends to a considerable extent on the chemical nature of each individual ion. Using an idealized membrane model found useful by earlier workers, values of the potential energy barrier created by image forces acting on various ions due to their charge and polarizability were calculated to determine ionic mobilities according to the Nernst-Planck equation. The agreement obtained between measurements of ionic mobilities in lipid bilayer membranes and theoretical predictions indicates that ionic polarizability is a possible origin of ionic selectivity in thin membranes.

The authors acknowledge the National Science Foundation for supporting the initial phases of this work by a Research Initiation Grant, NSF-GK-27892, and a fellowship for R.W.B. Computer expenses were provided for by the Dean of the School of Engineering, Stanford University.

References

1. Andersen, O.S., Fuchs, M. 1975. Potential energy barriers to ion transport within lipid bilayers: Studies with tetraphylborate. *Biophys. J.* **15**:795
2. Anderson, J.E., Jackson, H.W. 1974. Membrane-water partition coefficients of ions. Calculated effects of membrane thickness. *J. Phys. Chem.* **78**:2259
3. Barker, R.E., Jr., Thomas, C.R. 1964. Glass transition and ionic conductivity in cellulose acetate. *J. Appl. Phys.* **35**:87
4. Barrer, R.M., Rees, L.V.C. 1960. Energies of activation for self-diffusion of alkali metal ions in analcite. *Nature* **187**:768
5. Benz, R., Stark, G. 1975. Kinetics of macrotetralide-induced ion transport across lipid bilayer membranes. *Biochim. Biophys. Acta* **382**:27
6. Benz, R., Stark, G., Janko, K., Läuger, P. 1973. Valinomycin-mediated ion transport through neutral lipid membranes: Influence of hydrocarbon chain length and temperature. *J. Membrane Biol.* **14**:339
7. Bondi, A. 1968. Physical Properties of Molecular Crystals, Liquids and Glasses. pp. 453–468. Wiley, New York
8. Böttcher, C.J.F. 1973. Theory of Electric Polarization. Vol. I, p. 86. Elsevier Publishing Co., New York

9. Ciani, S., Laprade, R., Eisenman, G., Szabo, G. 1973. Theory for carrier-mediated zero-current conductance of bilayers extended to allow for nonequilibrium of interfacial reactions, spatially dependent mobilities and barrier shape. *J. Membrane Biol.* **11**:255
10. Cogan, U., Shinitzky, M., Weber, G., Nishida, T. 1973. Microviscosity and order in the hydrocarbon region of phospholipid and phospholipid-cholesterol dispersions determined with fluorescent probes. *Biochemistry* **12**:521
11. Coster, H.G.L., Smith, J.R. 1974. The molecular organization of bimolecular lipid membranes. A study of the low frequency Maxwell-Wagner impedance. *Biochim. Biophys. Acta* **373**:151
12. Fettiplace, R., Andrews, D.M., Haydon, D.A. 1971. The thickness, composition and structure of some lipid bilayers and natural membranes. *J. Membrane Biol.* **5**:277
13. Fuoss, R.M., Hirsch, E. 1960. Single ion conductances in non-aqueous solvents. *J. Amer. Chem. Soc.* **82**:1013
14. Galla, H.-J., Sackmann, E. 1974. Lateral diffusion in the hydrophobic region of membranes: Use of pyrene excimers as optical probes. *Biochim. Biophys. Acta* **339**:103
15. Gambale, F., Gliozzi, A., Robello, M. 1973. Determination of rate constants in carrier-mediated diffusion through lipid bilayers. *Biochim. Biophys. Acta* **330**:325
16. Gilkerson, W.R., Srivastava, K.K. 1961. The dielectric properties of tetra-*n*-butyl-ammonium picrate, bromide and tetraphenylboride in some polar solvents at 25 °C. *J. Phys. Chem.* **65**:272
17. Gilkerson, W.R., Stewart, J.C. 1961. Polarizabilities and molar volumes of a number of salts in several solvents at 25 °C. *J. Phys. Chem.* **65**:1465
18. Hall, J.E., Mead, C.A., Szabo, G. 1973. A barrier model for current flow in lipid bilayer membranes. *J. Membrane Biol.* **11**:75
19. Haydon, D.A., Hladky, S.B. 1972. Ion transport across thin lipid membranes: A critical discussion of mechanisms in selected systems. *Q. Rev. Biophys.* **5**:187
20. Hladky, S.B. 1974. The energy barriers to ion transport by nonactin across thin lipid membranes. *Biochim. Biophys. Acta* **352**:71
21. Hladky, S.B., Gordon, C.G.M., Haydon, D.A. 1974. Molecular mechanisms of ion transport in lipid membranes. *Annu. Rev. Phys. Chem.* **25**:11
22. Jacobsen, K., Wobschall, D. 1974. Rotation of fluorescent probes localized within lipid bilayer membranes. *Chem. Phys. Lipids* **12**:117
23. Ketterer, B., Neumcke, B., Läuger, P. 1971. Transport mechanism of hydrophobic ions through lipid bilayer membranes. *J. Membrane Biol.* **5**:225
24. Krasne, S., Eisenman, G. 1973. The molecular basis of ion selectivity. *In:* Membranes. A Series of Advances. G. Eisenman, editor. p. 277. Marcel Dekker, Inc., New York
25. Krasne, S., Eisenman, G., Szabo, G. 1971. Freezing and melting of lipid bilayers and the mode of action of monactin, valinomycin and gramicidin. *Science* **174**:412
26. LeBlanc, O.H., Jr. 1969. Tetraphenylborate conductance through lipid bilayer membranes. *Biochim. Biophys. Acta* **193**:350
27. LeBlanc, O.H., Jr. 1971. Effect of uncouplers of oxidative phosphorylation on lipid bilayer membranes: Carbonylcynanide *m*-chlorophenylhydrazone. *J. Membrane Biol.* **4**:227
28. Neumcke, B., Läuger, P. 1969. Non-linear electrical effects in lipid bilayer membranes. II. Integration of the generalized Nernst-Planck equations. *Biophys. J.* **9**:1160
29. Parsegian, A. 1969. Energy of an ion crossing a low dielectric membrane: Solutions to four relevant electrostatic problems. *Nature* **221**:844
30. Rosenberg, B., Bhowmik, B.B. 1969. Donor-acceptor complexes and the semiconductivity of lipids. *Chem. Phys. Lipids* **3**:109
31. Ryan, T.H., Koryta, J., Hofananova-Matjekova, A., Brezina, M. 1974. Polarography of alkali metal ion complexes of macrotetralides: Complex ion size and stability. *Anal. Lett.* **7**:335

32. Shinitzky, M., Barenholz, Y. 1974. Dynamics of the hydrocarbon layer in liposomes of lecithin and sphingomyelin containing dicetylphosphate. *J. Biol. Chem.* **249**:2652
33. Simon, W., Morf, W. E., Meier, P. Ch. 1973. Specificity for alkali and alkaline earth cations of synthetic and natural organic complexing agents in membranes. *Struct. Bonding (Berlin)* **16**:113
34. Smythe, W. R. 1968. Static and Dynamic Electricity. p. 22. McGraw-Hill, New York
35. Stark, G., Benz, R., Pohl, G. W., Janko, K. 1972. Valinomycin as a probe for the study of structural changes of black lipid membranes. *Biochim. Biophys. Acta* **266**:603
36. Stark, G., Ketterer, B., Benz, R., Läuger, P. 1971. The rate constants of valinomycin-mediated ion transport through thin lipid membranes. *Biophys. J.* **11**:981
37. Szabo, G. 1973. Location of cations complexed by neutral carriers in lipid bilayer membranes. *Biophys. J.* **15**:306a
38. Tredgold, R. H. 1973. Hydration energy and the transport of ions through membranes. *Biochim. Biophys. Acta* **323**:143
39. Vanderkooi, J. M., Callis, J. B. 1974. Pyrene. A probe of lateral diffusion in the hydrophobic region of membranes. *Biochemistry* **13**:4000
40. Vanderkooi, J., Fischkoff, S., Chance, B., Cooper, R. A. 1974. Fluorescent probe analysis of the lipid architecture of natural and experimental cholesterol-rich membranes. *Biochemistry* **13**:1589